Static Cavity Expansion Model for Partially Confined Targets

Y. Partom
Institute for Advanced Technology
The University of Texas at Austin

January 1996

19961209 001

IAT.R 0092

REPORT DOCUMENTATION PAGE

Form Approved
OMB NO. 0704-0188

1. AGENCY USE ONLY (Leave blank)	2. REPORT DATE January 1996	3. REPORT TYPE AND DATES COVERED Technical Report

4. TITLE AND SUBTITLE
Static Cavity Expansion Model for Partially Confined Targets

5. FUNDING NUMBERS
Contract # DAAA21-93-C-0101

6. AUTHOR(S)
Y. Partom

7. PERFORMING ORGANIZATION NAME(S) AND ADDRESS(ES)
Institute for Advanced Technology
The University of Texas at Austin
4030-2 W. Braker Lane, #200
Austin, TX 78759

8. PERFORMING ORGANIZATION REPORT NUMBER
IAT.R 0092

9. SPONSORING / MONITORING AGENCY NAME(S) AND ADDRESS(ES)
U.S. Army Research Laboratory
ATTN: AMSRL-WT-T
Aberdeen Proving Ground, MD 21005-5066

10. SPONSORING / MONITORING AGENCY REPORT NUMBER

11. SUPPLEMENTARY NOTES
The view, opinions and/or findings contained in this report are those of the author(s) and should not be considered as an official Department of the Army position, policy, or decision, unless so designated by other documentation.

12a. DISTRIBUTION / AVAILABILITY STATEMENT
Approved for public release; distribution unlimited.

12b. DISTRIBUTION CODE
A

13. ABSTRACT (Maximum 200 words)

The cavity expansion model (CEM), originally proposed as an indentation theory, has been used extensively to estimate the resistance of targets to long rod penetration. In the classical model the target is infinite and the cavity is opened up from zero radius. In previous work we applied the classical approach to laterally finite targets and we ran into difficulty. The resistance came out as decreasing with cavity radius. To circumvent the difficulty we introduced an averaging scheme with a free parameter to be determined from computer simulations. In this work we use a different approach, we open up the cavity from a finite radius. We first propose the concept that the target penetration resistance is the limit of stability of the cavity. We then apply this concept to estimate the resistance of partially confined targets. We do this for both cylindrical and spherical cavities. Comparing the model solutions to computer simulation results reported in [2] we find good agreement for the spherical CEM, but not for the cylindrical CEM.

14. SUBJECT TERMS
Cavity Expansion Model, long rod penetration

15. NUMBER OF PAGES
15

16. PRICE CODE

17. SECURITY CLASSIFICATION OF REPORT Unclassified	18. SECURITY CLASSIFICATION OF THIS PAGE Unclassified	19. SECURITY CLASSIFICATION OF ABSTRACT Unclassified	20. LIMITATION OF ABSTRACT UL

Contents

List of Figures

Static Cavity Expansion Model for Partially Confined Targets

Yehuda Partom

Abstract

The cavity expansion model (CEM), originally proposed as an indentation theory, has been used extensively to estimate the resistance of targets to long rod penetration. In the classical model the target is infinite and the cavity is opened up from zero radius. In previous work we applied the classical approach to laterally finite targets and we ran into difficulty. The resistance came out as decreasing with cavity radius. To circumvent the difficulty we introduced an averaging scheme with a free parameter to be determined from computer simulations.

In this work we use a different approach, we open up the cavity from a **finite radius**. We first propose the concept that the target penetration resistance is the **limit of stability** of the cavity. We then apply this concept to estimate the resistance of partially confined targets. We do this for both cylindrical and spherical cavities.

Comparing the model solutions to computer simulation results reported in [2] we find good agreement for the spherical CEM, but not for the cylindrical CEM.

1.0   Introduction

In [1] we applied the static cavity expansion model (CEM) in cylindrical symmetry to estimate the efficiency of lateral self-confinement in metal and ceramic targets. In [2] we calibrated and validated the results obtained in [1] using computer simulations.

Our approach in [1] and [2] was along the lines of the original CEM [3] namely, evaluating the internal pressure P(a) needed to open a cavity from zero radius. For a finite outside radius, b, we found that P(a) was not constant but decreased with the cavity radius "a." We therefore averaged P(a) over a certain range of "a" and defined this average to be the target resistance. We calibrated the averaging range from the results of computer simulations.

In what follows we use a different approach. We first show that the value of P(a) obtained from the classical CEM (b → ∞) is actually the **limit of stability** of a finite radius cavity expanded by internal pressure. We then use this insight and evaluate the limit of stability for finite b. We regard the limit of stability P_ℓ to be the target penetration resistance.

We find that P_0 depends on b_0/a_0 (where a_0, b_0 are the initial inside and outside radii). Identifying a_0 with the projectile radius we obtain good agreement with computer simulations for a spherical cavity but only qualitative agreement for a cylindrical cavity.

In Section 2 we explain the concept of the limit of stability. Section 3 provides the analysis for a cylindrical cavity, and Section 4 provides the analysis for a spherical cavity. Chapter 5 shows the model solutions for penetration resistance as a function of the degree of confinement and compares this to computer simulation results.

2.0   Limit of Stability

To explain the limit of stability concept we evaluate the elasto-plastic cavity expansion from a finite initial cavity a_0.

2.1.   Cylindrical Cavity

The elastic field is:

$$u = \frac{\beta Y}{2G} \frac{c^2}{r},$$

$$\sigma_r = -\beta Y \frac{c^2}{r^2},$$

$$\sigma_\theta = \beta Y \frac{c^2}{r^2},$$

(1)

$$\sigma_r - \sigma_\theta = -2\beta Y \frac{c^2}{r^2},$$

where:

u = radial displacement

σ_r, σ_θ = radial and tangential stress components

$\beta = \sqrt{3}/3$

Y = yield stress and flow stress

G = shear modulus

c = elastic-plastic boundary radius

r = radial coordinate

and where at r = c we have:

$$\sigma_r - \sigma_\theta = -2\beta Y, \tag{2}$$

which follows from the von-Mises yield surface and from [3]:

$$\sigma_z = \frac{1}{2}(\sigma_r + \sigma_\theta), \tag{3}$$

where σ_z = axial stress component. At r = c we have:

$$u(c) = \frac{\beta Y}{2G} c, \tag{4}$$

$$\sigma_r(c) = -\beta Y.$$

From mass conservation (ignoring density changes) we have:

$$c^2 - a^2 = [c - u(c)]^2 - a_0^2, \tag{5}$$

$$\therefore \frac{c^2}{a^2} \cong \frac{G}{\beta Y}\left(1 - \frac{a_0^2}{a^2}\right).$$

The plastic field is:

$$\sigma_r = 2\beta Y\left(-\frac{1}{2} + \ln\frac{r}{c}\right), \tag{6}$$

and the cavity wall pressure is:

$$P(a) = \beta Y\left\{1 + \ln\left[\frac{G}{\beta Y}\left(1 - \frac{a_0^2}{a^2}\right)\right]\right\}. \tag{7}$$

We see that as a_0 goes to zero, P(a) increases to a limit value:

$$P_\ell = \begin{array}{c} P(a) \\ a_0 \to 0 \end{array} = \beta Y\left(1 + \ell n\frac{G}{\beta Y}\right), \tag{8}$$

which is the classical result for cylindrical cavity expansion.

3

The P(a) curve from (7) is shown in Figure 1 and discussed below together with the spherical cavity results.

2.2. Spherical Cavity

The elastic field is:

$$u = \frac{Y}{6G} \frac{c^3}{r^2},$$

$$\sigma_r = -\frac{2}{3}Y \cdot \frac{c^3}{r^3}, \tag{9}$$

$$\sigma_\theta = \sigma_\varphi = \frac{1}{3}Y \cdot \frac{c^3}{r^3},$$

$$\sigma_r - \sigma_\theta = -Y \cdot \frac{c^3}{r^3},$$

where (r, θ, φ) are the spherical coordinates.

At $r = c$ we have:

$$u(c) = \frac{Y}{6G}c,$$

$$\sigma_r(c) = -\frac{2}{3}Y, \tag{10}$$

$$(\sigma_r - \sigma_\theta)(c) = -Y.$$

From mass conservation (and no density change) we have:

$$c^3 - a^3 = [c - u(c)]^3 - a_0{}^3,$$

$$\therefore \frac{c^3}{a^3} \cong \frac{2G}{Y}\left(1 - \frac{a_0{}^3}{a^3}\right). \tag{11}$$

The plastic field is:

$$\sigma_r = 2Y\left(-\frac{1}{3} + \ln\frac{r}{c}\right),$$

(12)

and the cavity wall pressure is:

$$P(a) = \frac{2}{3}Y\left\{1 + \ln\left[\frac{2G}{Y}\left(1 - \frac{a_0^3}{a^3}\right)\right]\right\},$$

(13)

from which we get the limit value:

$$P_\ell = \mathop{P(a)}_{(a_0 \to 0)} = \frac{2}{3}Y\left(1 + \ln\frac{2G}{Y}\right).$$

(14)

The P(a) curve from (13) is also shown in Figure 1.

2.3. Limit of Stability and Penetration Resistance

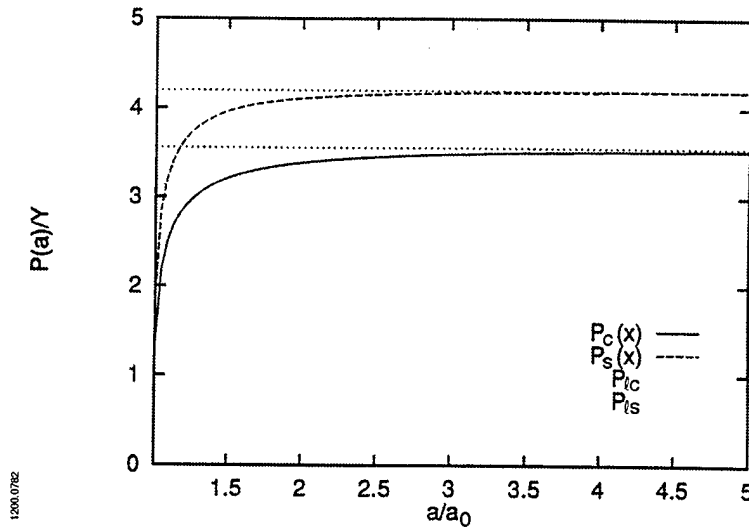The cavity expansion results obtained for G/Y = 100 are shown in Figure 1.

Figure 1. Cavity expansion (a/a$_0$), in an infinite domain, as a function of scaled internal pressure (P(a)/Y), for cylindrical and spherical symmetry. The horizontal asymptotes are the limits of stability of the cavity. P_c is given by (7), P_s by (13), $P_{\ell c}$ by (8) and $P_{\ell s}$ by (14). G/Y = 100.

We see that as long as $P(a/a_o) < P_\ell$, the cavity is statically stable with a radius "a." At $P = P_\ell$ the cavity can grow indefinitely, quasistatically (with zero velocity). Also, because a/a_0 is infinite when a finite cavity is opened from zero radius, P_ℓ is identical to the penetration resistance obtained from the classical CEM [3]. This provides a different way of looking at penetration resistance obtained from CEMs: penetration resistance is the internal pressure on the cavity wall that would make the cavity expand indefinitely, at zero velocity. For $P > P_\ell$, the cavity wall is accelerated by the internal pressure.

In [1] and [2] we used the CEM to estimate the penetration resistance of partially confined targets. Using the classical approach (opening a finite cavity from zero radius) we found that the internal pressure needed to open the cavity to a radius "a" was a decreasing function of "a." To extract a penetration resistance value from $P(a)$ we averaged it over the range $0 < a < a_r$, where a_r was calibrated from computer simulation results.

By applying the limit of stability approach to cavity expansion in a finite domain we can avoid the arbitrariness of the averaging approach.

3.0   Cylindrical Cavity Expansion, Finite a_0 and b_0

The elastic field is:

$$u = \frac{\beta Y}{2G} r \left(\frac{c^2}{r^2} + \frac{G}{\lambda + G} \cdot \frac{c^2}{b^2} \right),$$

$$\sigma_r = -\beta Y \left(\frac{c^2}{r^2} - \frac{c^2}{b^2} \right),$$

$$\sigma_\theta = \beta Y \left(\frac{c^2}{r^2} + \frac{c^2}{b^2} \right), \tag{15}$$

$$\sigma_z = \beta Y \frac{\lambda}{\lambda + G} \cdot \frac{c^2}{b^2},$$

$$\sigma_r - \sigma_\theta = -2\beta Y \cdot \frac{c^2}{r^2},$$

$$P = -\beta Y \cdot \frac{K}{\lambda + G} \cdot \frac{c^2}{b^2},$$

where:

λ = Lame's modulus,

K = Bulk modulus.

The elastic moduli ratios in (15) are:

$$\frac{\lambda}{\lambda + G} = 2v,$$

$$\frac{G}{\lambda + G} = 1 - 2v, \qquad (16)$$

$$\frac{K}{\lambda + G} = \frac{2}{3}(1 + v),$$

where v = Poisson's ratio.

and at $r = c$ we have:

$$u(c) = \frac{\beta Y}{2G} c \left[1 + (1 - 2v)\frac{c^2}{b^2} \right],$$

$$\qquad (17)$$

$$\sigma_r(c) = -\beta Y \left(1 - \frac{c^2}{b^2} \right).$$

The plastic field solution is:

$$\sigma_r = -\beta Y \left(1 - \frac{c^2}{b^2} + \ln\frac{c^2}{r^2} \right), \qquad (18)$$

so that:

$$P(a) = \beta Y \left(1 - \frac{c^2}{b^2} + \ln\frac{c^2}{a^2} \right). \qquad (19)$$

From mass conservation we have (as in Section 2.1):

$$c^2 - a^2 = [c - u(c)]^2 - a_0^2, \tag{20}$$

$$\frac{c^2}{a^2} \cong \frac{1}{2}\left(1 - \frac{a_0^2}{a^2}\right) \cdot \frac{c}{u(c)},$$

$$\therefore \frac{c^2}{a^2} = \frac{G}{\beta Y} \cdot \frac{1 - a_0^2/a^2}{1 + (1 - 2v) \cdot \dfrac{c^2}{b^2}}. \tag{21}$$

Also, at r = b we have:

$$b = b_0 + u(b),$$

$$\tag{22}$$

$$u(b) = \frac{c^2}{b^2} \cdot \frac{\beta Y}{G}(1 - v),$$

so that:

$$\frac{c}{a} = \frac{\dfrac{b_0}{a_0} \cdot \dfrac{a_0}{a} \cdot \dfrac{c}{b}}{1 - \dfrac{\beta Y}{G} \cdot (1 - v) \cdot \dfrac{c^2}{b^2}}. \tag{23}$$

Equations (21) and (23) are nonlinear simultaneous equations in c/a and c/b. Substituting c/a from (23) into (21) we obtain a quadratic equation in c^2/b^2 which can be solved analytically for given b_0/a_0 and a/a_0. Finally, substituting into (19) gives P(a) for given b_0/a_0 and a/a_0.

When the elastic-plastic interface reaches the outside boundary we have:

$$c = b,$$

$$P(a) = \beta Y \ln \frac{b^2}{a^2}, \tag{24}$$

$$\frac{b^2}{a^2} = \frac{G}{\beta Y} \cdot \frac{1 - a_0^2/a^2}{2(1 - v)}.$$

But from (22):

8

$$\frac{b}{b_0} = \frac{1}{1 - \frac{\beta Y}{G}(1 - \nu)} . \tag{25}$$

Eliminating b from the last of (24) and (25) we get:

$$\left(\frac{a}{a_0}\right)^2 = 1 + \left(\frac{b_0}{a_0}\right)^2 \cdot \frac{2(1-\nu) \cdot \frac{\beta Y}{G}}{\left[1 - (1-\nu) \cdot \frac{\beta Y}{G}\right]^2} \quad \text{for } c = b. \tag{26}$$

For $a > a_{c=b}$ the second of (24) still holds, and b^2/a^2 is obtained from mass conservation:

$$b^2 - a^2 = b_0^2 - a_0^2, \tag{27}$$

$$\frac{b^2}{a^2} = 1 + \frac{a_0^2}{a^2}\left(\frac{b_0^2}{a_0^2} - 1\right).$$

Results for $P(a)/Y$ as a function of a/a_0, for $G/Y = 100$, $\nu = 0.3$, and for different values of b_0/a_0, are shown in Figure 2. We see that the curves rise to a peak and then drop. The value of $P(a)$ at the peak is the limit of stability pressure P_ℓ. We see that P_ℓ increases with b_0/a_0 and that the corresponding a/a_0 value increases. In Chapter 5 we further discuss these results together with the spherical cavity results obtained in Chapter 4.
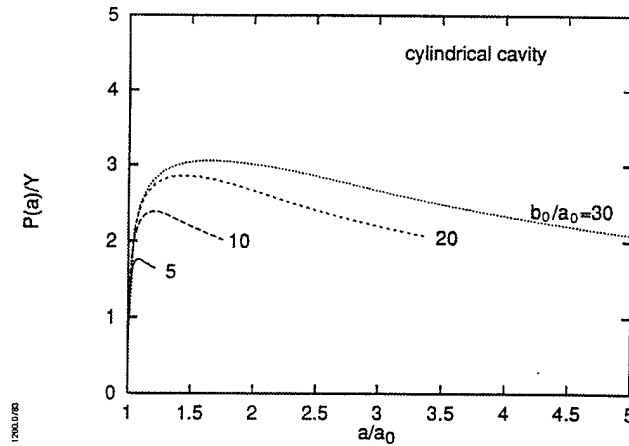

Figure 2. Cylindrical cavity expansion (a/a_0), in a finite domain, as a function of the scaled internal pressure ($P(a)/Y$), for $G/Y = 100$ and $\nu = 0.3$. The different curves are for different values of b_0/a_0.

4.0 Spherical Cavity Expansion (finite a_0 and b_0)

The elastic field is:

$$u = \frac{Y}{6G} r \left(\frac{c^3}{r^3} + 2 \cdot \frac{1-2v}{1+v} \cdot \frac{c^3}{b^3} \right),$$

$$\sigma_r = -\frac{2}{3} Y \left(\frac{c^3}{r^3} - \frac{c^3}{b^3} \right),$$

$$\sigma_\theta = \frac{2}{3} Y \left(\frac{1}{2} \cdot \frac{c^3}{r^3} + \frac{c^3}{b^3} \right), \qquad (28)$$

$$\sigma_r - \sigma_\theta = -Y \cdot \frac{c^3}{r^3},$$

$$P = -\frac{2}{3} Y \cdot \frac{c^3}{b^3},$$

and at $r = c$ we have:

$$u(c) = \frac{Y}{6G} c \left(1 + 2 \cdot \frac{1-2v}{1+v} \cdot \frac{c^3}{b^3} \right),$$

$$\sigma_r(c) = -\frac{2}{3} Y \left(1 - \frac{c^3}{b^3} \right). \qquad (29)$$

The plastic field solution is:

$$\sigma_r = -\frac{2}{3} Y \left(1 - \frac{c^3}{b^3} + \ln \frac{c^3}{r^3} \right), \qquad (30)$$

so that:

$$P(a) = \frac{2}{3} Y \left(1 - \frac{c^3}{b^3} + \ln \frac{c^3}{a^3} \right). \qquad (31)$$

10

From mass conservation we have:

$$c^3 - a^3 = [c - u(c)]^3 - a_0^3,$$

(32)

$$\frac{c^3}{b^3} \cong \frac{1}{3}\left(1 - \frac{a_0^3}{a^3}\right) \cdot \frac{c}{u(c)},$$

$$\frac{c^3}{a^3} = \frac{2G}{Y} \cdot \frac{(1 - a_0^3/a^3)}{1 + 2 \cdot \frac{1 - 2\nu}{1 + \nu} \cdot \frac{c^3}{b^3}}.$$

(33)

Also, at r = b we have:

$$b = b_0 + u(b),$$

(34)

$$u(b) = \frac{Y}{2G} \cdot \frac{c^3}{b^2} \cdot \frac{1 - \nu}{1 + \nu},$$

so that:

$$\frac{c}{a} = \frac{\dfrac{b_0}{a_0} \cdot \dfrac{a_0}{a} \cdot \dfrac{c}{b}}{1 - \dfrac{Y}{2G} \cdot \dfrac{1 - \nu}{1 + \nu} \cdot \dfrac{c^3}{b^3}}.$$

(35)

Equations (33) and (35) are nonlinear simultaneous equations in c/a and c/b. Substituting c/a from (35) into (33) we get a cubic equation in c^3/b^3 which can be solved numerically with a standard bisection routine. Finally, substituting back into (31) gives P(a) for given b_0/a_0 and a/a_0.

When the elastic-plastic interface reaches the outside boundary we have:

$$c = b,$$

$$\frac{b^3}{a^3} = \frac{1 - a_0^3/a^3}{\dfrac{3}{2} \cdot \dfrac{Y}{G} \cdot \dfrac{1 - \nu}{1 + \nu}},$$

(36)

$$P(a) = \frac{2}{3}Y\ln\frac{b^3}{a^3}.$$

But from (34):

$$\frac{b}{b_0} = \frac{1}{1 - \dfrac{Y}{2G} \cdot \dfrac{1-\nu}{1+\nu}}. \tag{37}$$

Eliminating b from the second of (36) and (37) we get:

$$\left(\frac{a}{a_0}\right)^3 = 1 + \left(\frac{b_0}{a_0}\right)^3 \cdot \frac{\dfrac{3}{2} \cdot \dfrac{Y}{G} \cdot \dfrac{1-\nu}{1+\nu}}{\left(1 - \dfrac{Y}{2G} \cdot \dfrac{1-\nu}{1+\nu}\right)^3} \quad \text{for } c = b. \tag{38}$$

For $a > a_{c=b}$ the third of (36) still holds, and b^3/a^3 is obtained from mass conservation:

$$b^3 - a^3 = b_0^3 - a_0^3,$$

$$\frac{b^3}{a^3} = 1 + \left(\frac{a_0}{a}\right)^3 \left(\frac{b_0^3}{a_0^3} - 1\right). \tag{39}$$

Results for $P(a)/Y$ as a function of a/a_0, for $G/Y = 100$, $\nu = 0.3$, and for different values of b_0/a_0, are shown in Figure 3. The curves are similar in nature to those shown in Figure 2 for the cylindrical cavity.
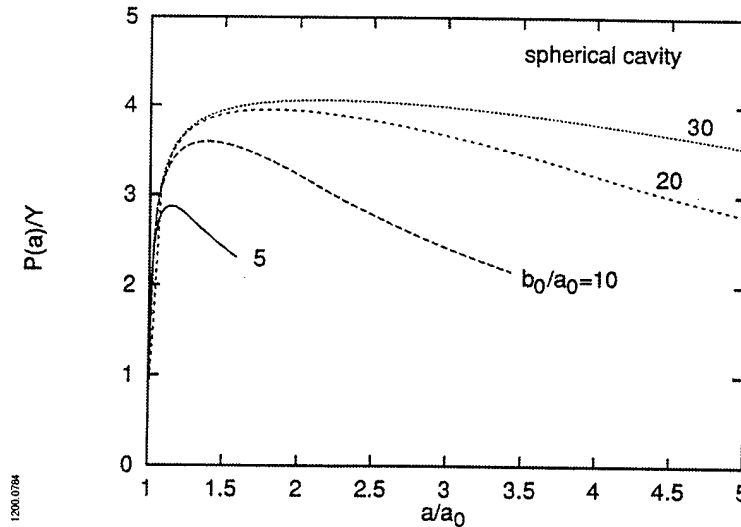

Figure 3. Spherical cavity expansion (a/a_0), in a finite domain, as a function of the scaled internal pressure ($P(a)/Y$), for $G/Y = 100$, $\nu = 0.3$. The different curves are for different values of b_0/a_0.

12

5.0 Penetration Resistance Results and Conclusions

As explained in the introduction, the peaks of the curves in Figures 2 and 3 are the limits of stability of the cavity, in terms of the scaled internal pressure (P_ℓ/Y). In Figure 4 we show P_ℓ/Y as a function of b_0/a_0 for cylindrical and spherical cavities.
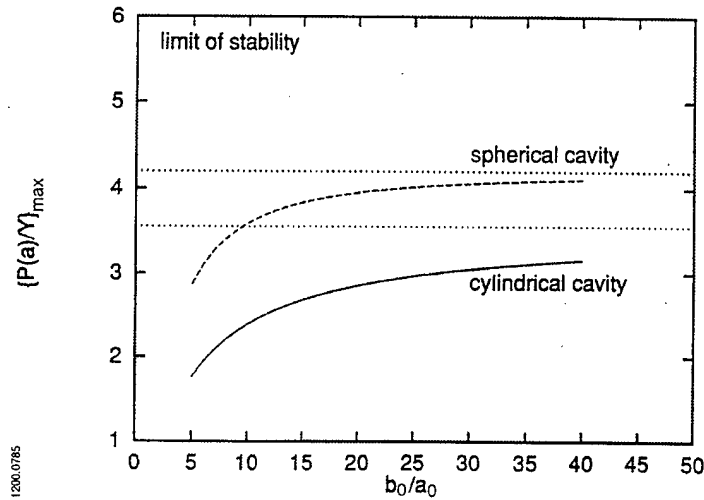

Figure 4. Limit of stability (maxima of P(a)/Y versus a/a$_0$ curves) as a function of b$_0$/a$_0$ for cylindrical and spherical cavities. G/Y = 100, ν = 0.3. Asymptotes are the same as in Figure 1.

We see that the spherical cavity curve approaches its asymptote faster that the cylindrical cavity curve. In Figure 5 we show that the same results only normalized to their asymptotic values (P_ℓ for $b_0 \rightarrow \infty$). We also identify P_ℓ as the penetration resistance R and denote the asymptotic values by R_{inf}.
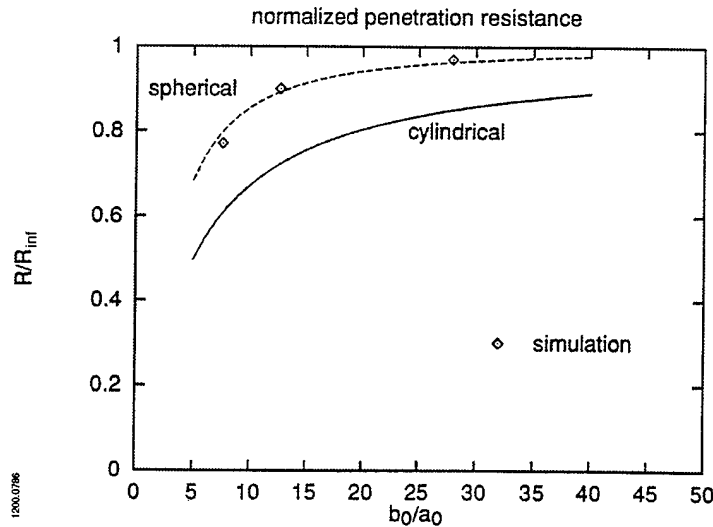

Figure 5. Same as in Figure 4 but normalized to values at infinite b$_0$; also, P$_\ell$ is identified with penetration resistance R. Points are from simulations with steel targets in [2] assuming that D$_t$/D$_p$ $\equiv$ b$_0$/a$_0$.

13

We also put on Figure 5 the results of numerical simulation with steel targets from [2]. In doing that we assumed that D_t/D_p in the simulation (where D_t = target diameter and D_p = projectile diameter) is identical with b_0/a_0 in the CEM. We see that the simulation points are quite close to the spherical cavity curve. (For steel, $G/Y = 100$ and $\nu = 0.3$ is a good approximation, and the sensitivity to those parameters is low.)

We conclude that:

- The limit of stability approach is an appropriate tool for estimating penetration resistance of partially confined targets.

- The spherical CEM is better suited to model penetration resistance than the cylindrical CEM.

Acknowledgment

References

1. Y. Partom, "Efficiency of Lateral Self Confinement in Metal and Ceramic Targets," IAT.R 0019, April 1993.

2. Y. Partom and D. L. Littlefield, "Validation and Calibration of a Lateral Confinement Model for Long Rod Penetration," IAT.R 0035, February 1994.

3. R. F. Bishop, R. Hill, and N. F. Mott, "The Theory of Indentation and Hardness Tests," *Proc. Phys. Soc.*, vol. 57, p. 148, 1945.

Distribution List

Administrator
Defense Technical Information Center
Attn: DTIC-DDA
8725 John J. Kingman Road, Ste 0944
Ft. Belvoir, VA 22060-6218

Dr. Stephan Bless
Institute for Advanced Technology
The University of Texas at Austin
4030-2 W. Braker Lane, Suite 200
Austin, TX 78759

Director
US Army Research Lab
ATTN: AMSRL OP SD TA
2800 Powder Mill Road
Adelphi, MD 20783-1145

W. deRosset
U.S. Army Research Laboratory
Attn: AMSRL-WT-TC
Aberdeen Prvg Grd, MD 21005-5066

Director
US Army Research Lab
ATTN: AMSRL OP SD TL
2800 Powder Mill Road
Adelphi, MD 20783-1145

Mr. Michael Forrestal
Sandia National Laboratory
Division 1922
P.O. Box 5800
Albuquerque, NM 87185

Director
US Army Research Lab
ATTN: AMSRL OP SD TP
2800 Powder Mill Road
Adelphi, MD 20783-1145

Dr. Joe Foster
Air Force Armament & Technology Lab
AFATL/MNW
Eglin AFB, FL 32542

Army Research Laboratory
AMSRL-CI-LP
Technical Library 305
Aberdeen Prvg Grd, MD 21005-5066

K. Frank
U.S. Army Research Laboratory
Attn: AMSRL-WT-TD
Aberdeen Prvg Grd, MD 21005-5066

Dr. Charles Anderson, Jr.
Southwest Research Institute
Engineering Dynamics Department
P.O. Box 28510
San Antonio, TX 78228-0510

Edward Schmidt
U.S. Army Research Laboratory
Attn: AMSRL-WT-PB
Aberdeen Prvg Grd, MD 21005-5066

T. Bjerke
Director
U.S. Army Research Laboratory
Attn: AMSRL-WT-TC
Aberdeen Prvg Grd, MD 21005-5066

Dr. Joseph Sternberg
Physics Dept.
Naval Postgraduate School
Monterey, CA 93943

15